




University of  
Stavanger

Faculty of Science and Technology

## MASTER'S THESIS

Study program/Specialization: Master in Robotics and signal processing	Spring semester, 2021  Open
Writer: Eivind Berge Mesna	 ..... (Writer's signature)
Faculty supervisor: Arnfinn A. Eielsen	
External supervisor(s):	
Thesis title: Improved displacement estimation in homodyne Michelson interferometers	
Credits (ECTS): 30	
Key words: Michelson interferometer, interferometry, Heydemann, optics, displacement estimation, Extended Kalman Filter	Pages: 31 + enclosure: 0  Stavanger, 15th of July 2021 Date/year





Faculty of Science and Technology

Department of Electrical Engineering and Computer Science

# Improved displacement estimation in homodyne Michelson interferometers

Master's Thesis in Robotics and Signal processing  
by

Eivind Berge Mesna

Supervisor

Arnfinn A. Eielsen

15<sup>th</sup> of July 2021

# Abstract

A Michelson interferometer is a victim to lots of displacement noise that changes over time and distorts the measurement making them less accurate. There are some types of estimators for these distortions, but they usually claim a lot of computer power and it is therefore a need for investigating methods using less computationally dependent filters for these estimates. In this paper an estimation method for estimating the unknown parameters of a Homodyne Michelson interferometer system using the Extended Kalman filter is suggested.

A good mathematical model of an interferometer based off Jones calculus is implemented into Simulink to design and verify the results of the filter and compared with data obtained with a Michelson interferometer learning kit from ThorLabs.

The designed state space model doesn't estimate the amplitude and the quadrature error but shows good results when taking the final estimated movement of the measured object.

The mathematical model used in Simulink is well described as well as the state space model used for in the Extended Kalman Filter. This paper shows only one approach on how to use the EKF for this purpose and there are still improvements to be done on this approach.

Parallel with this project a bachelor thesis have been written with a more practical approach on how to use the interferometer (Nesjø & Kvamme, 2021).

## Figure table

Figure 1: The LIGO facilities LIGO Hanford and LIGO Livingston located in Washington and Louisiana (USA) respectively (LIGO Caltech, n.d.) .....	8
Figure 2: A simple block diagram of a Michelson interferometer (Eielsen A. A., 2021). .....	9
Figure 3: Constructive and destructive interference .....	12
Figure 4: The Michelson Interferometer educational kit and its components from Thorlabs (Thorlabs, n.d.) .....	13
Figure 5: Test results from heating the aluminium rod .....	14
Figure 6: Measurements taken and then corrected with Heudemann method (Heydemann, 1981). The amplitude and offset of the uncorrected data are corrected in this figure for a better presentation .....	16
Figure 7: The Extended Kalman Loop (MathWorks, 2021) .....	18
Figure 8: Simulated data with noise and estimated data .....	23
Figure 9: Unwrapping of the two output signals (Nesjø & Kvamme, 2021).....	24
Figure 10: Last 100 samples for $\Delta L$ of the data in Figure 8, with and without unwrapping .....	24
Figure 11: First 250 samples for $\Delta L$ of the data in Figure 8, with and without unwrapping .....	25
Figure 12: Guesses for initial values of the states .....	25
Figure 13: Different initial values for $\alpha_1$ and $\alpha_2$ and how they stabilize over time .....	26
Figure 14: Measured data used in this demonstration .....	27
Figure 15: The output signals plotted up against each other .....	28
Figure 16: Estimated movement with both the EKF algorithm and the Heydemann method .....	29
Figure 17: The derivatives of the estimated values using EKF and the Heydemann method.....	29

# Equation table

Equation 1: The Jones matrix for $-\pi/4$ rotation of light (right hand), with polarizing filters on input and output.....	10
Equation 2: Jones matrices for mirrors with and without displacement.....	10
Equation 3: Jones matrices for polarizing filter.....	10
Equation 4: Representation of $45^\circ$ polarized light going through a $\lambda/4$ WP giving a right hand circular polarization (Loughridge & Abramovitch, 2013).....	11
Equation 5: The Jones matrix used for a waveplate of $\lambda/8$ (Hecht, 2001).....	11
Equation 6: Interference equation according to Loughridge and Abramovitch (Loughridge & Abramovitch, 2013). $A$ is amplitude, $\omega$ is the frequency, $k = 2\pi/\lambda$ , $L_{ref}$ is the length to the reference mirror and back, and $L_{meas}$ is the same for the moving mirror. ....	12
Equation 7: Electromagnetic wave of light described with Jones vector (Hecht, 2001).....	15
Equation 8: Jones vector .....	15
Equation 9: Least square equation for the distorted ellipse (Heydemann, 1981).....	16
Equation 10: Equation for calculating parameters A-E (Ersbo, 2018).....	16
Equation 11: Parameters A-E equations (Ersbo, 2018).....	16
Equation 12: Parameters $r$ , $p$ , $q$ and $\alpha$ for a distorted ellipse.....	17
Equation 13: The system and measurement equations.....	17
Equation 14: Interference and quadrature signal realised with Jones calculus.....	19
Equation 15: Jones vector for polarized light in x direction.....	19
Equation 16: Interference signal with polarized light as input. This is calculated with Equation 14 and Equation 15. ....	19
Equation 17: Irradiance with two light components (Nesjø & Kvamme, 2021). Where $c$ = the speed of light and $\epsilon_0$ = vacuum permittivity .....	19
Equation 18: Output signal with polarized light as input and no noise. ....	19
Equation 19: Quadrature signal .....	20
Equation 20: Generalization for the quadrature signals (Eielsen A. A., 2018).....	20
Equation 21: Generalized output signal without error in WP.....	21
Equation 22: Augmented state vector .....	21
Equation 23: Measurement equation .....	22
Equation 24: State transition equations and matrix.....	22
Equation 25: Covariance matrix .....	22

## Abbreviations and key variables

Abbreviation	Definition
LB	Laser beam
TM	Target mirror
RM	Reference mirror
KM	Kalman Filter
EKF	Extended Kalman Filter
BS	Beam splitter
PBS	Polarized beam splitter
WP	Wave plate
PD	Photo detector

Variables	Description
$v_1$ and $v_2$	The measured output signals from the interferometer
$\alpha_1$ and $\alpha_2$	The sinusoidal offset
$\beta_1$ and $\beta_2$	The gain displacement
$e_\varphi$	Quadrature error
$\theta$	Phase of the interference signal
$E_{0x}$ and $E_{0y}$	Electromagnetic field in x and y axis
$\lambda$	Light wavelength
$\omega$	Light frequency

## Acknowledgments

I will use this opportunity to give my thanks to the University of Stavanger and my supervisor Arnfinn Eielsen for making it possible to realise this thesis with facilities and necessary help. I would also like to thank Thomas Nesjø and Magnus Kvamme, whom wrote their bachelor thesis on the same subject, for great cooperation.

A special thanks to family and friends for motivating me to finish the project while my closest family have had a tough time the past few months. This would not have been possible without the extra motivation.

And last but not least I want to thank the guys at the Mikrolab for great company and the high spirit throughout the whole semester.



# Contents

1	Introduction.....	8
2	The interferometer.....	9
2.1	Isolator.....	9
2.2	Mirrors and Beam splitters.....	10
2.3	Waveplate .....	10
2.4	Photo detectors.....	11
2.5	Interference and fringes.....	11
2.6	The setup.....	13
3	Methods .....	15
3.1	Jones calculus .....	15
3.2	The Heydemann Method .....	15
3.3	Extended Kalman Filter .....	17
4	Model and simulation .....	19
5	Estimation.....	21
5.1	State space model .....	21
6	Results and discussion.....	23
6.1	Simulation.....	23
6.2	Using actual data.....	27
6.3	Real-time implementation .....	29
7	Conclusion .....	30
8	Bibliography.....	31

# 1 Introduction

A Homodyne Michelson interferometer is a measurement device using a polarized laser beam to measure changes in distance with extremely high precision. By having a stationary mirror as reference and a moving mirror as the changing distance the laser beam is split towards the two mirrors that reflect the laser beams back, creating an interference signal. By using a wave plate, we can obtain a quadrature signal to get direction of the movement. Change in the interference signal is dependent on the movement of the moving mirror and the wavelength of the laser. We know that from constructive interference (high amplitude) to destructive interference (low amplitude) the moving mirror have moved  $\pi$  radians of the laser's wavelength. With a known wavelength we can therefore calculate the movement of the mirror down to nano meter precision. A typical laser used in interferometry is a He-Ne laser with a wavelength at 632.8 nm. In this thesis a laser with a wavelength at about 532 nm is used due to expenses.

Laser interferometry is a widely used measurement method mainly used to measure displacement in length. The best-known measurement device using laser interferometry is the LIGO facilities in the US. This is used to measure gravitational waves from space by having 4 km long tunnels in each direction (LIGO's Interferometer). Laser interferometry is also used in a quite smaller scale such as in CNC machines for better precision.



*Figure 1: The LIGO facilities LIGO Hanford and LIGO Livingston located in Washington and Louisiana (USA) respectively (LIGO Caltech, n.d.)*

One of the bigger issues with an interferometer is the displacement occurring by misalignments and natural error in its components. This will cause an output signal that differentiate over time and the interferometer needs to be calibrated for keeping its high precision. The commonly used method for calibrating an interferometer is the Heydemann method (Heydemann, 1981). Using the least square of a data set, the output signal can be batch calibrated, but this will quickly drift and cause problems for later measurements and measurements over longer periods. Then a new calibration is needed. It is therefore some ongoing research for methods in calibrating the interferometer while doing measurements without using a lot of computer power.

The goal in this thesis is to learn how to use a Michelson interferometer, make a realistic mathematical model in Matlab/Simulink and use the simulation model to make an algorithm to estimate the displacement issues we can experience using an interferometer. The proposed method is using the Extended Kalman Filter. This thesis have been working parallel with a bachelor thesis that have a more practical approach to the use of the interferometer (Nesjø & Kvamme, 2021)

# 2 The interferometer

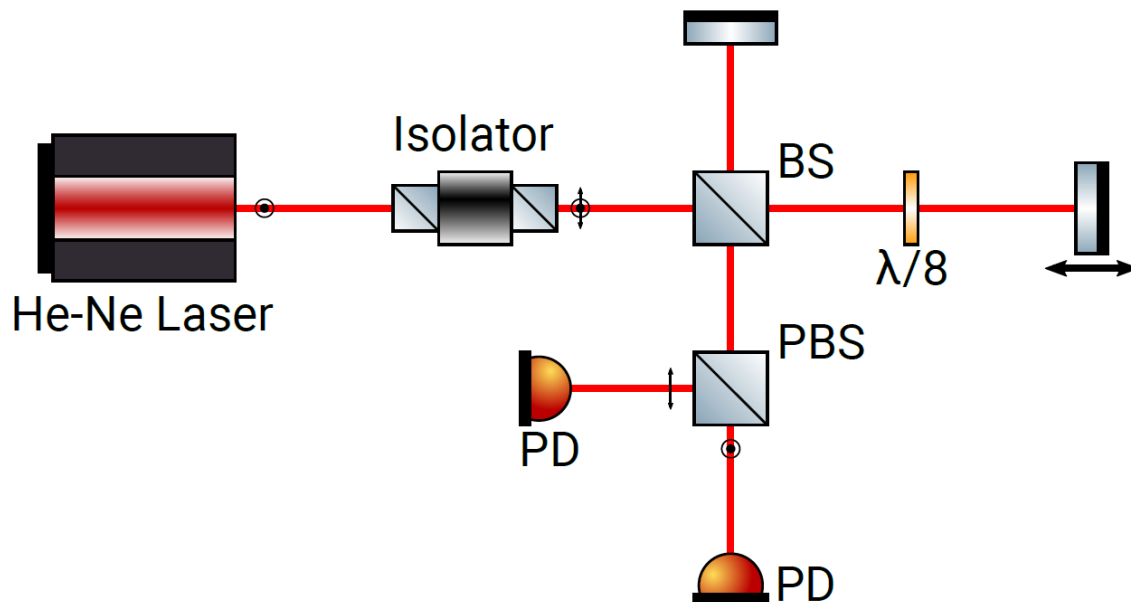


Figure 2: A simple block diagram of a Michelson interferometer (Eielsen A. A., 2021).

The interferometer is built by putting together components with different optical properties to do one job. It starts with a laser that sends out a vertically polarised light (x direction) into an isolator that rotates the polarisation  $45^\circ$  or  $\frac{\pi}{2}$  radians. Then the beam is split in two directions with a beam splitter (BS). One beam reflects off a reference mirror (stationary) and back to the beam splitter. The other beam goes through a waveplate, reflects off a target mirror (movable) and through the waveplate again on its way back to the beam splitter. The two beams then combine in the beam splitter and this creates interference. The interference signal is then split in a polarized beam splitter (PBS) and sent to two separate photo detectors, one measuring the interference signal polarized vertically, and the other horizontally. The waveplate is there to create a quadrature interference signal to be able to determine direction.

By splitting the beam and not using two lasers we are sure that the wavelength of the two laser beams creating the interference are the same. This is important in creating good interference.

## 2.1 Isolator

The isolator has two main functions, rotating the light  $\frac{\pi}{4}$  radians and preventing the laser beam to go back into the laser to prevent noise. The  $\frac{\pi}{4}$  rotation of the light is not necessary since the laser itself can just be rotated, but it is necessary for an easy set-up of the polarizing filters and waveplate later.

An optical isolator consists of three parts, an input polarizing filter, a faraday rotator and an output polarizing filter. The light is polarized in a vertical orientation, rotated  $\frac{\pi}{4}$  radians and goes through the output polarizing filter oriented in  $\frac{\pi}{4}$  radians. When some light reflects back at the isolator, the light

going the opposite direction will be rotated the same direction and therefore blocked by the input polarizing filter since it has now a total rotation of  $\frac{\pi}{2}$  radians.

$$J_I(\theta) = \frac{1}{2} \begin{bmatrix} 1 & -1 \\ -1 & 1 \end{bmatrix} \begin{bmatrix} \cos(\theta) & \sin(\theta) \\ -\sin(\theta) & \cos(\theta) \end{bmatrix} \begin{bmatrix} 1 & 0 \\ 0 & 0 \end{bmatrix} \Rightarrow J_I\left(-\frac{\pi}{4}\right) = \frac{1}{2} \begin{bmatrix} \sqrt{2} & 0 \\ \sqrt{2} & 0 \end{bmatrix}$$

Equation 1: The Jones matrix for  $-\pi/4$  rotation of light (right hand), with polarizing filters on input and output

## 2.2 Mirrors and Beam splitters

A mirror is simply a reflecting surface that ideally reflects 100% of the light, and it will at the same time mirror the signal. In a Michelson interferometer two mirrors are used, a stationary reference mirror and a movable target mirror. The movement of the target mirror will give a phase shift relative to the target mirror when the two beams later interfere.

$$J_{RM} = \begin{bmatrix} -1 & 0 \\ 0 & -1 \end{bmatrix} \quad J_{TM} = \begin{bmatrix} -e^{i\theta} & 0 \\ 0 & -e^{i\theta} \end{bmatrix}$$

Equation 2: Jones matrices for mirrors with and without displacement

As the name says, the beam splitter splits the beams in two directions. An ideal beam splitter splits half of the light in one direction, and the other half in the other direction. The beam splitter is also used to create interference when the light beams reflected off the mirrors comes back to the beam splitter. The interference signal will also leave in two directions, so the interference signal will ideally have half its energy.

The polarizing beam splitter is a normal beam splitter with polarizing filters, one vertical and one horizontal, on its output. This is used to measure the light in the x-axis and y-axis independently.

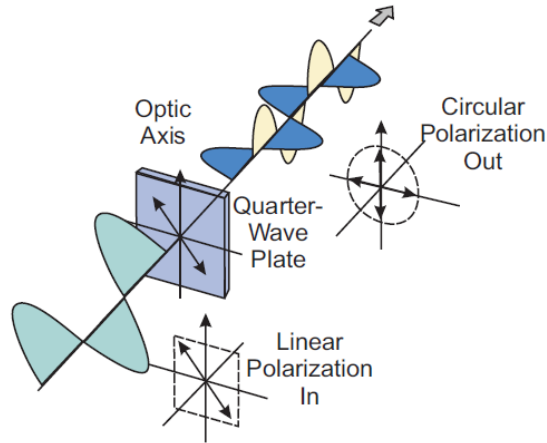
$$J_{HP} = \begin{bmatrix} 1 & 0 \\ 0 & 0 \end{bmatrix} \quad J_{VP} = \begin{bmatrix} 0 & 0 \\ 0 & 1 \end{bmatrix} \quad J_{\theta P} = \begin{bmatrix} \cos^2(\theta) & \cos(\theta)\sin(\theta) \\ \cos(\theta)\sin(\theta) & \sin^2(\theta) \end{bmatrix}$$

Equation 3: Jones matrices for polarizing filter

## 2.3 Waveplate

The waveplate is crucial in determining the direction and length from one measurement to another. What the waveplate does is to slow the light (retards) in one axis and fastens it in the perpendicular axis. To generate a quadrature signal the waveplate has to have a phase shift of  $\frac{\lambda}{8}$  since the light will pass through the waveplate twice. When light has a quadrature signal from x- to y-axis it is called circular polarized light. This gives a total of  $\frac{\lambda}{4}$  phase shift between x- and y-axis. In this case a waveplate with vertical fast axis is used (y-axis).

The WP used in this project operates in the range of 550-750 nm and is therefore not the right fit for the 532 nm laser. This will by default not give a circular polarized output signal, but a more elliptical output. For this thesis it's good enough.



Equation 4: Representation of 45° polarized light going through a  $\lambda/4$  WP giving a right hand circular polarization (Loughridge & Abramovitch, 2013)

$$J_R^V\left(\frac{\lambda}{8}\right) = \begin{bmatrix} e^{i\frac{\pi}{8}} & 0 \\ 0 & e^{-i\frac{\pi}{8}} \end{bmatrix} = e^{i\frac{\pi}{8}} \begin{bmatrix} 1 & 0 \\ 0 & e^{-i\frac{\pi}{4}} \end{bmatrix}$$

Equation 5: The Jones matrix used for a waveplate of  $\lambda/8$  (Hecht, 2001).

## 2.4 Photo detectors

A photodetector (PD) is a light receiving diode that transfer the light received into current. The signal received is called irradiance and are given by the light intensity over an area  $\left(\frac{W}{m^2}\right)$ . Irradiance is mathematically explained in Equation 17 in Model and simulation 4 below.

The PD are of the type SM1PD1B from ThorLabs and are connected to a transimpedance amplifier circuit to convert the current produced into voltage, this circuit will also work as a low pass filter if the operational amplifier used isn't faster than the PD. More about the transimpedance amplifier circuit can be read in the bachelor thesis (Nesjø & Kvamme, 2021).

## 2.5 Interference and fringes

Interference is a phenomenon occurring when two waves of the same wavelength collide (interfere). Depending on the relative phase of the two waves the interference will create constructive interference, destructive interference or something in between. Constructive interference happens when the two waves are in phase and the amplitude will then double. Destructive interference happens when the two waves has a relative phase shift of  $\pi$  radians, and the two waves will zero out each other.

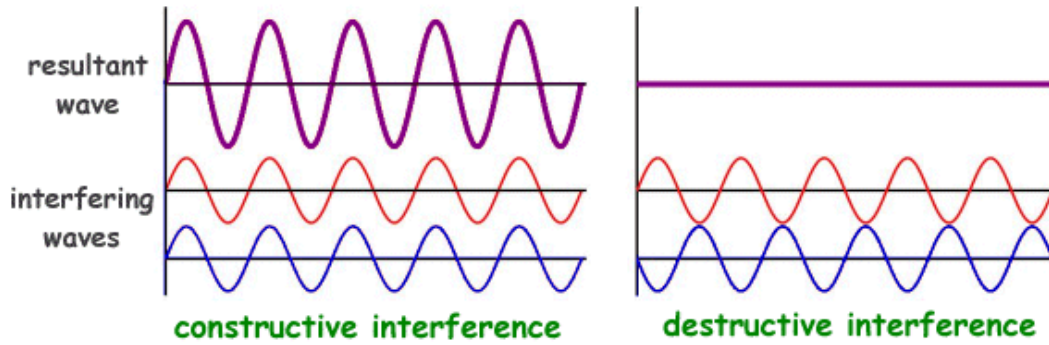


Figure 3: Constructive and destructive interference

The interference in an interferometer happens when the two light beams hit the BS and therefore the alignments of the beams are crucial for creating a good interference signal. The alignment of the beams can be adjusted on the reference mirror.

Equation 6 gives a mathematical approach to an interference signal in a Michelson interferometer.

$$E_{tot}(t) = \frac{A}{4} [\cos(kL_{ref} - \omega t + \varphi) + \cos(kL_{meas} - \omega t + \varphi)]$$

Equation 6: Interference equation according to Loughridge and Abramovitch (Loughridge & Abramovitch, 2013).  $A$  is amplitude,  $\omega$  is the frequency,  $k = \frac{2\pi}{\lambda}$ ,  $L_{ref}$  is the length to the reference mirror and back, and  $L_{meas}$  is the same for the moving mirror.

## 2.6 The setup

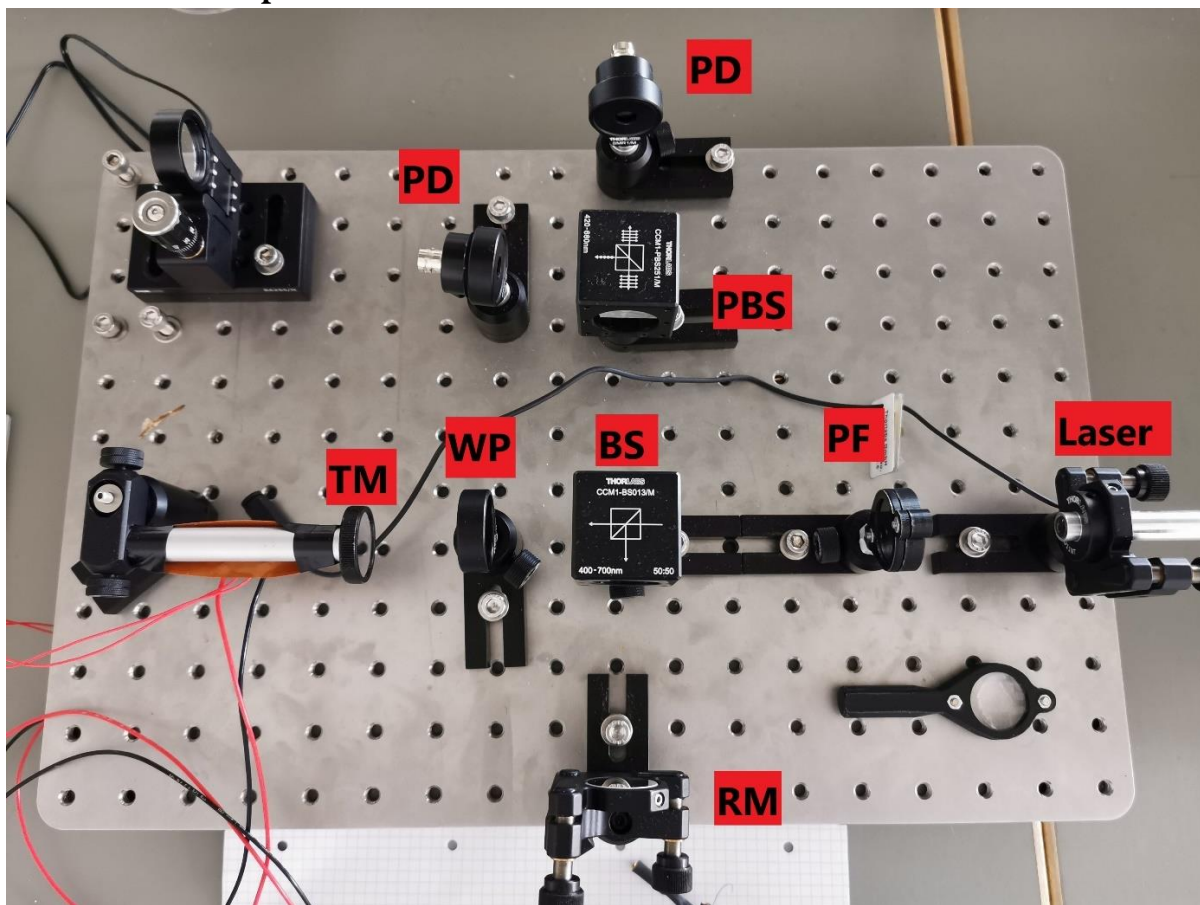


Figure 4: The Michelson Interferometer educational kit and its components from Thorlabs (Thorlabs, n.d.)

For this thesis an educational kit from Thorlabs (Thorlabs, n.d.) have been used. With it comes all the components needed for this setup except an extra photo detector (PD) and the waveplate (WP). The waveplate were bought from Union Optic.

On the output a transimpedance amplifier circuit were connected to convert the current from the PD's to voltage (Nesjø & Kvamme, 2021).

Since an isolator is too expensive for a simple setup like this, the laser first goes through a polarizing filter tilted 45°. The rest of the interferometer is given a little misalignment so that the laser beam doesn't reflect into the laser, which might have given a disturbance or damage the laser. These misalignments make the interference harder to align and will be easier misaligned by movement in the TM.

To get test results the TM were fitted on an aluminium rod. The rod was heated up and would then expand, causing the TM to move towards the WP. There is also an option to use a TM moved manually. This mirror can be seen on the top left in Figure 4.

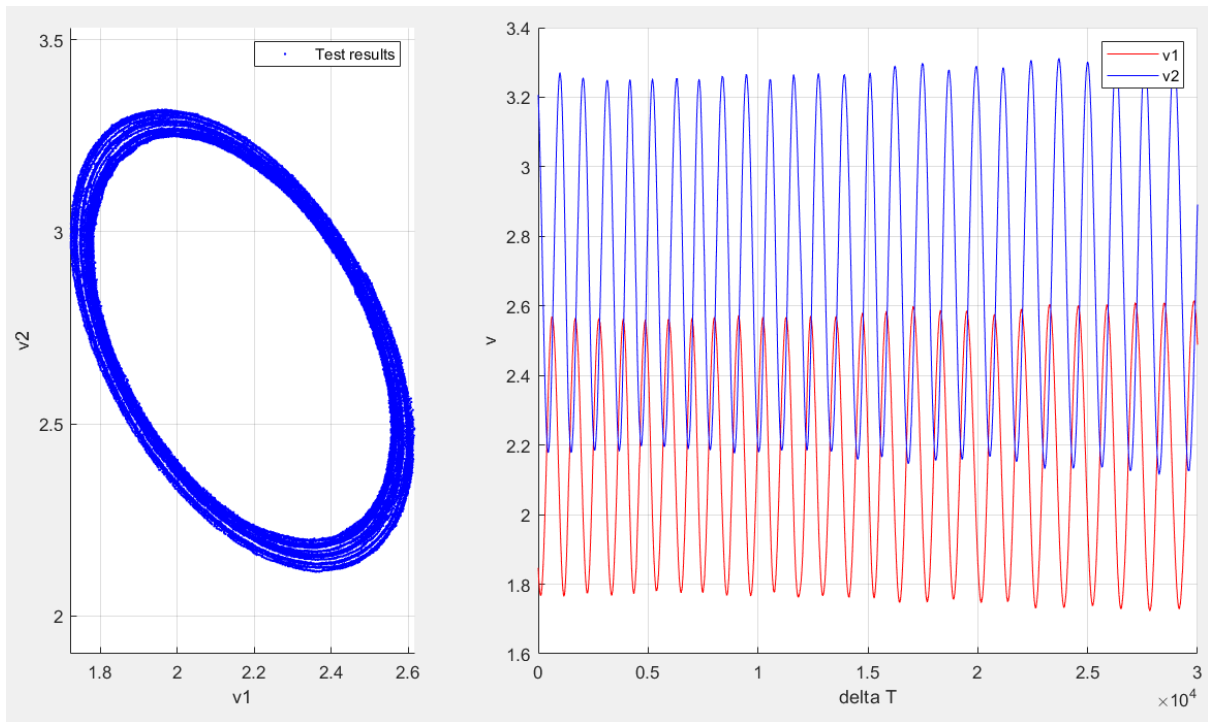


Figure 5: Test results from heating the aluminium rod

As shown in Figure 5, the output signal from this setup has some displacement from the start and this is changing over time. This displacement issue is explained in chapter 4 Model and simulation.



# 3 Methods

## 3.1 Jones calculus

When dealing with polarized light in mathematics Jones calculus is a way of describing it. The electromagnetic wave can be described as

$$\vec{E} = \vec{E}_0 e^{i(\vec{k}\cdot\vec{r}-\omega t)} \Rightarrow \begin{bmatrix} E_{0x} e^{i\phi x} \\ E_{0y} e^{i\phi y} \\ 0 \end{bmatrix} e^{i(\vec{k}\cdot\vec{z}-\omega t)}$$

*Equation 7: Electromagnetic wave of light described with Jones vector (Hecht, 2001)*

The last exponential part of Equation 7 describe the direction of the light going in z-direction, and we can therefore look at just the x- and y-axis in an simulation given the frequency don't change. For simplification, the frame of reference will change when the direction of the light change. Then we have the Jones vector as following

$$\begin{bmatrix} E_{0x} e^{i\phi x} \\ E_{0y} e^{i\phi y} \end{bmatrix}$$

*Equation 8: Jones vector*

The  $E_{0x}$  is the amplitude in the x-axis (horizontal) and the  $e^{i\phi x}$  is the phase shift of the x-axis. The same goes for y-axis.

By using Jones vector and matrices a mathematical model can be made in Simulink by multiplying the different matrices for the optical component with each other. The Jones matrices for the optical components used is given in chapter 2 The interferometer.

## 3.2 The Heydemann Method

In an ideal world with no noise or misalignments the two signals detected by the photodetectors will make a perfect quadrature signal. Plotting them against each other will then make a perfect circle around origin, and taking the arctangent of signal 2 divided by signal 1 will give us the displacement angle on the target mirror used in Equation 2. Knowing the wavelength, we can easily calculate the movement.

The world is not ideal, and a Michelson interferometer is a victim for a lot of different noise. This noise is typically a not perfect wave plate, laser wave drift, amplitude drift/differences, movement of air particles etc. Combined these disturbances will make the circle moves away from the origin and become an ellipse, which makes trouble for calculating the movement of the target mirror.

The Heydemann method (Heydemann, 1981) is a widely used method to calibrate the output signal from the interferometer to make a circle around origin. By moving the target mirror and collecting data, the least square method can then be used to calibrate the noise, as shown in (Heydemann, 1981).

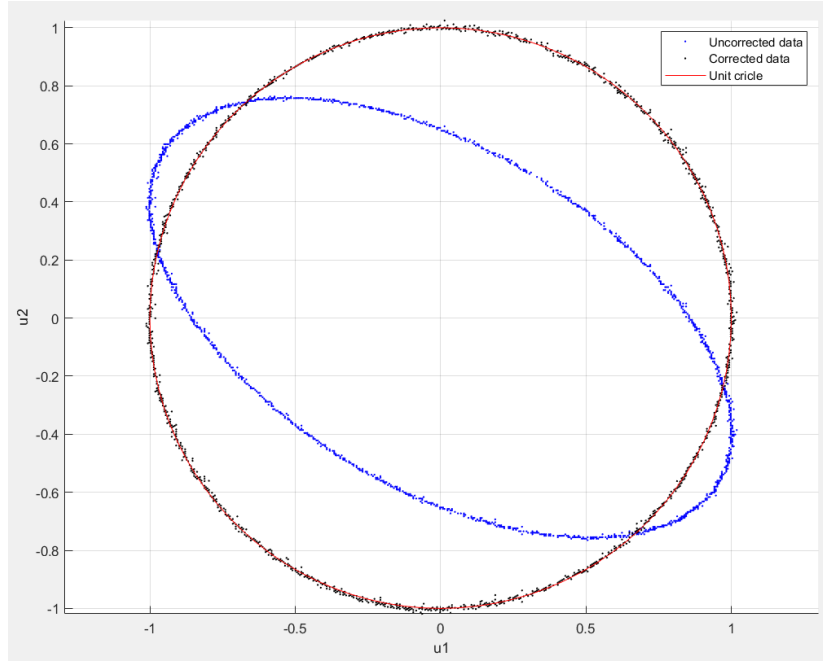


Figure 6: Measurements taken and then corrected with Heydemann method (Heydemann, 1981). The amplitude and offset of the uncorrected data are corrected in this figure for a better presentation

The Heydemann method uses 4 variables to describe the distorted ellipse.  $\alpha$  as the reference signal quadrature error,  $r$  as the channel gain ratio and for the offset in the two channels,  $p$  and  $q$  is used for  $u_1$  and  $u_2$  respectively.

Heydemann uses Equation 9 to describe the distorted ellipse

$$Au_1^{d2} + Bu_2^{d2} + Cu_1^d u_2^d + Du_1^d + Eu_2^d = 1$$

Equation 9: Least square equation for the distorted ellipse (Heydemann, 1981)

Using linear algebra, we can find the parameters with Equation 10

$$\begin{bmatrix} A \\ B \\ C \\ D \\ E \end{bmatrix} = (Y^T Y)^{-1} Y^T [1_1 \quad 1_2 \quad \dots \quad 1_N], \quad Y = [u_1^{d2} \quad u_2^{d2} \quad u_1^d u_2^d \quad u_1^d \quad u_2^d]$$

Equation 10: Equation for calculating parameters A-E (Ersbo, 2018)

The parameters are described in Equation 11

$$\begin{aligned} A &= (R^2 \cos^2 \alpha - p^2 - r^2 q^2 - 2rpq \sin \alpha)^{-1} \\ B &= Ar^2 \\ C &= 2Ar \sin \alpha \\ D &= -2A(p + rq \sin \alpha) \\ E &= -2Ar(rq + p \sin \alpha) \end{aligned}$$

Equation 11: Parameters A-E equations (Ersbo, 2018)

This then gives the parameters  $r$ ,  $p$ ,  $q$  and  $\alpha$

$$\begin{aligned}
r &= \left(\frac{B}{A}\right)^{\frac{1}{2}} \\
p &= \frac{2BD - EC}{C^2 - 4AB} \\
q &= \frac{2AE - DC}{C^2 - 4AB} \\
\alpha &= \sin^{-1}\left(\frac{-C}{\sqrt{4AB}}\right)
\end{aligned}$$

Equation 12: Parameters  $r$ ,  $p$ ,  $q$  and  $\alpha$  for a distorted ellipse

With the parameters from Equation 12, the corrected ellipse can be found with

$$\begin{aligned}
u_1 &= u_1^d - p \\
u_2 &= \frac{1}{\cos\alpha}(u_1^d - p)\sin\alpha + ru_2^d - q
\end{aligned}$$

### 3.3 Extended Kalman Filter

Without going too much into detail on how the Extended Kalman filter (EKF) works since this can be easily obtained on the web, here is a brief explanation and how Simulink use it.

As the name indicate the Extended Kalman filter is an extended version of the Kalman Filter (KM). The problem with the KM is that it only works on linear systems and linear systems don't exist in the real world (Simon, 2006). The output of the interferometer is highly nonlinear and will change over time, therefore it will be difficult to linearise the system and a KM can't be used. That's why the EKF is more appropriated for this task.

The EKF works mostly in the same way as the KF. In the linear KF the Jacobian of the state equations are in use as the transition function, but in an EKF the transition function is changing and dependent on what state the system is in. Therefore, a transition function needs to be specified and a Jacobian of this transition function needs to be calculated.

In Simulink there is an Extended Kalman Filter block that will be used. This uses the discrete-time EKF and has the possibility to calculate the Jacobian matrices numerically. In Figure 7 the Extended Kalman loop used in Simulink is represented with it's predict and update equations.

$$\begin{aligned}
x_{k+1} &= f_k(x_k, u_k, w_k) \\
y_k &= h_k(x_k, v_k) \\
w_k &\sim (0, Q_k) \\
v_k &\sim (0, R_k)
\end{aligned}$$

Equation 13: The system and measurement equations

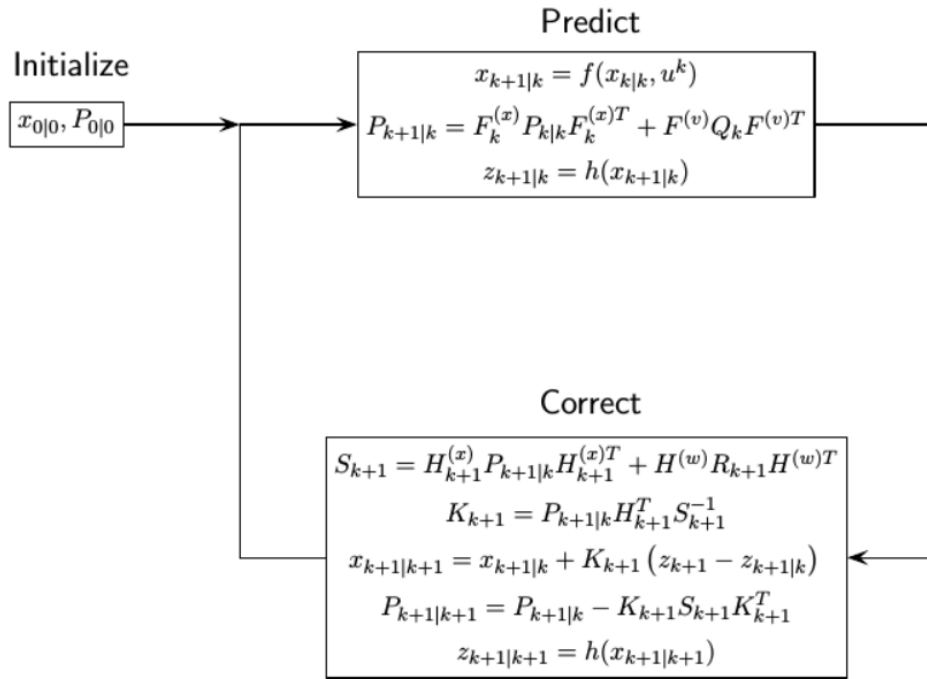


Figure 7: The Extended Kalman Loop (MathWorks, 2021)

# 4 Model and simulation

The simulation for this paper is done in Simulink. The mathematics is realised with Jones calculus explained in chapter 3.1. The model uses Jones vector to create two cosine waves going the speed of light and has a wavelength of 532 nm. Then all the Jones matrices for the components are added as Simulink blocks.

The first essential part is to make a quadrature signal and interference. This is done by multiplying the matrices for the components (2) in the right order, from right to left.

$$\begin{bmatrix} v_x \\ v_y \end{bmatrix} = \frac{1}{2} \begin{bmatrix} -1 & 0 \\ 0 & -1 \end{bmatrix} \frac{1}{2} \begin{bmatrix} \sqrt{2} & 0 \\ \sqrt{2} & 0 \end{bmatrix} \begin{bmatrix} E_{0x} e^{i\phi x} \\ E_{0y} e^{i\phi y} \end{bmatrix} e^{i(\vec{k}\cdot\vec{z}-wt)} \\ + \frac{1}{2} \begin{bmatrix} e^{i\frac{\pi}{8}} & 0 \\ 0 & e^{-i\frac{\pi}{8}} \end{bmatrix} \begin{bmatrix} -e^{i\theta} & 0 \\ 0 & -e^{i\theta} \end{bmatrix} \begin{bmatrix} e^{i\frac{\pi}{8}} & 0 \\ 0 & e^{-i\frac{\pi}{8}} \end{bmatrix} \frac{1}{2} \begin{bmatrix} \sqrt{2} & 0 \\ \sqrt{2} & 0 \end{bmatrix} \begin{bmatrix} E_{0x} e^{i\phi x} \\ E_{0y} e^{i\phi y} \end{bmatrix} e^{i(\vec{k}\cdot\vec{z}-wt)}$$

Equation 14: Interference and quadrature signal realised with Jones calculus.

The jones vector in Equation 14 will give two components, one in the x-axis and one in the y-axis. The z-axis is always the direction the light is going.

$$\begin{bmatrix} E_{0x} e^{i\phi x} \\ E_{0y} e^{i\phi y} \end{bmatrix} = \begin{bmatrix} e^{i\varphi} \\ 0 \end{bmatrix} = \begin{bmatrix} 1 \\ 0 \end{bmatrix}_{\varphi=0}$$

Equation 15: Jones vector for polarized light in x direction

$$\begin{bmatrix} v_x \\ v_y \end{bmatrix} = -\frac{\sqrt{2}}{4} \cdot \left( \begin{bmatrix} 1 \\ 1 \end{bmatrix} + \begin{bmatrix} e^{i(\theta+\frac{\pi}{4})} \\ e^{i(\theta-\frac{\pi}{4})} \end{bmatrix} \right) e^{i(\vec{k}\cdot\vec{z}-wt)}$$

Equation 16: Interference signal with polarized light as input. This is calculated with Equation 14 and Equation 15.

The photodetectors are not quick enough to integrate the frequency of the light waves and therefore detect the light intensity over a given area. This is called irradiance  $\left(\frac{W}{m^2}\right)$  and is given by the following equation

$$I = \frac{c\varepsilon_0}{2} E_{net}^2 = \frac{c\varepsilon_0}{2} (|\vec{E}_1|^2 + |\vec{E}_2|^2 + 2\vec{E}_1 \cdot \vec{E}_2)$$

Equation 17: Irradiance with two light components (Nesjø & Kvamme, 2021). Where  $c$  = the speed of light and  $\varepsilon_0$  = vacuum permittivity

Where  $\vec{E}_1$  and  $\vec{E}_2$  are the electromagnetic field of the light given by Equation 7

The photodetectors are working as lowpass filters and will keep the DC component. The output signal we are left with is

$$\begin{bmatrix} v_x \\ v_y \end{bmatrix} = -\frac{\sqrt{2}}{4} \cdot \left( \begin{bmatrix} 1 \\ 1 \end{bmatrix} + \begin{bmatrix} e^{i(\theta+\frac{\pi}{4})} \\ e^{i(\theta-\frac{\pi}{4})} \end{bmatrix} \right)$$

Equation 18: Output signal with polarized light as input and no noise.

The output signal in Equation 18 has two components, one in the x axis and one in the y axis. The y axis lags behind the x axis with  $\frac{\pi}{2}$  and this gives a quadrature signal on the output with  $\theta$  as input. If we only look at the real values, the output signal can be written as in Equation 19.

$$\begin{bmatrix} v_x \\ v_y \end{bmatrix} = \begin{bmatrix} \cos(\theta) \\ \sin(\theta) \end{bmatrix}$$

Equation 19: Quadrature signal

The signal won't be without noise and misalignments. As explained in 3.2 the noise will distort and move around the circle obtained when dividing  $v_y$  by  $v_x$ . Equation 20 shows the quadrature signal with added noise. This will make the circle to an ellipse, make it bigger/smaller and move it away from origin.

$$\begin{bmatrix} v_x \\ v_y \end{bmatrix} = \begin{bmatrix} \alpha_x + \beta_x \cdot \cos(kL) + e_x \\ \alpha_y + \beta_y \cdot \sin(kL + e_\varphi) + e_y \end{bmatrix}$$

Equation 20: Generalization for the quadrature signals (Eielsen A. A., 2018)

$\alpha$  is the account for any bias,  $\beta$  is the difference in gain,  $e_\varphi$  is the quadrature error often given by a not perfect waveplate and the uncertainty of the wavelength, and  $e$  is the process noise from the photo detectors. The constant  $k$  is given by  $k = \frac{2\pi}{\lambda}$ , where in this paper  $\lambda = 532$  nm. The misalignments  $\alpha$  and  $\beta$  can be added to the model by multiplying and adding on the output signal, but for a more realistic simulation there can be added bias in the beam splitters, laser etc., and there can added gain blocks that can be represented as loss in reflectance in each component. The quadrature error  $e_\varphi$  can be added in the jones matrices for the wave plate in Equation 14 (see 2.3).

The discrete time system of the output signal is given the displacement between each measurement.

$$\Delta L = (\eta + L)_1 - (\eta + L)_0$$

Where  $L$  is the phase shift in meters and since the laser beam goes back and forth  $L$  is double the size of the movement of the target mirror. When multiplying  $k$  and  $L$  in Equation 20 what we are left with is the phase shift  $\theta$ . This make the measurement discrete and therefore can be used in the EKF by Simulink.

# 5 Estimation

As discussed in 3.2 the interferometer is a victim to a lot of displacement and noise that can change over time. In this chapter a method will be proposed for estimating the displacement of the output signal of the Michelson interferometer.

Taking Equation 20 into account we have two output signals

$$v_1 = \alpha_1 + \beta_1 \cdot \cos(\theta(t)) + e_1$$

$$v_2 = \alpha_2 + \beta_2 \cdot \sin(\theta(t) + e_\varphi) + e_2$$

The quadrature error ( $e_\varphi$ ) between the two signals is normally due to a not perfect WP or/and drift in the laser's wavelength. This is normally not changing that much over time, so let's say this is a known constant for simplification. This constant is a delay in one of the output signal and can be found practically by sampling a movement on the TM over more than one period of the wavelength, plotting the two output signals and delaying one of the output so that  $v_2$  lags  $\frac{\pi}{2}$  behind  $v_1$ . We can then remove  $e_\varphi$  from the equation and what we are left with is

$$v_1 = \alpha_1 + \beta_1 \cdot \cos(\theta(t)) + e_1$$

$$v_2 = \alpha_2 + \beta_2 \cdot \sin(\theta(t)) + e_2$$

*Equation 21: Generalized output signal without error in WP*

where  $e_1$  and  $e_2$  is the process noise. The variables we then want to estimate is  $\alpha_1$ ,  $\alpha_2$ ,  $\beta_1$  and  $\beta_2$ . These variables are also changing over time, but not very quick. To predict the parameters of a system the unknown parameters can be added into an augmented vector as explained by Dan Simon in Optimal State Estimation page 422 (Simon, 2006).

## 5.1 State space model

The state of the interferometer is the phase shift given from the movement of the target mirror. This can be represented with the phase  $\theta(k)$  and the derivative  $\dot{\theta}(k)$ . The measurements are a cosine and a sine output of this phase and we don't really care about the phase, but only the parameters of the output. To make this easier the state of the system is set to  $\cos(\theta(k))$  and  $\sin(\theta(k))$ . The derivatives of these states can then be given by each other. The augmented state vector is then

$$x_k = \begin{bmatrix} x_1 \\ x_2 \\ x_3 \\ x_4 \\ x_5 \\ x_6 \end{bmatrix} = \begin{bmatrix} \cos(\theta_k) \\ \sin(\theta_k) \\ \beta_1 \\ \beta_2 \\ \alpha_1 \\ \alpha_2 \end{bmatrix}$$

*Equation 22: Augmented state vector*

With the measurement equations being as follow

$$v_{(1)k} = \alpha_1 + \beta_1 \cdot \cos(\theta_k) + v_k = x_3 \cdot x_1 + x_5$$

$$v_{(2)k} = \alpha_1 + \beta_1 \cdot \cos(\theta_k) + v_k = x_4 \cdot x_2 + x_6$$

We get the following measurement matrix

$$y_k = \begin{bmatrix} v_1 \\ v_2 \end{bmatrix} = \begin{bmatrix} x_3 \cdot x_1 + x_5 \\ x_4 \cdot x_2 + x_6 \end{bmatrix} + v_k$$

Equation 23: Measurement equation

Then there are the state transition equations for  $x_1$  and  $x_2$ . Since  $\dot{x}_1 = -x_2$  and  $\dot{x}_2 = x_1$  this will not be that complicated. But there is a bias in amplitude that makes these two statements not true. The proposed solution for this is shown in Equation 24.

$$x_{k+1} = \begin{bmatrix} \cos(\theta_{k+1}) \\ \sin(\theta_{k+1}) \\ \beta_1 \\ \beta_2 \\ \alpha_1 \\ \alpha_2 \end{bmatrix} = \begin{bmatrix} x_1 - x_2 \cdot \frac{x_3 + x_4}{2} \cdot k \\ x_2 + x_1 \cdot \frac{x_3 + x_4}{2} \cdot k \\ x_3 \\ x_4 \\ x_5 \\ x_6 \end{bmatrix} = \begin{bmatrix} 1 & -k \cdot \frac{x_3 + x_4}{2} & 0 & 0 & 0 & 0 \\ k \cdot \frac{x_3 + x_4}{2} & 1 & 0 & 0 & 0 & 0 \\ 0 & 0 & 1 & 0 & 0 & 0 \\ 0 & 0 & 0 & 1 & 0 & 0 \\ 0 & 0 & 0 & 0 & 1 & 0 \\ 0 & 0 & 0 & 0 & 0 & 1 \end{bmatrix}$$

Equation 24: State transition equations and matrix

The Jacobians is set to be calculated numerically since Simulink has the option to do so. When it comes to the covariance matrix this is a diagonal matrix with the covariance rate for each state on its diagonal. This is tuned so the rate of change of each state is as desired. A typical covariance matrix after tuning is

$$Q_{cov} = \begin{bmatrix} 0.1 & 0 & 0 & 0 & 0 & 0 \\ 0 & 0.1 & 0 & 0 & 0 & 0 \\ 0 & 0 & 0.001 & 0 & 0 & 0 \\ 0 & 0 & 0 & 0.001 & 0 & 0 \\ 0 & 0 & 0 & 0 & 0.0001 & 0 \\ 0 & 0 & 0 & 0 & 0 & 0.0001 \end{bmatrix}$$

Equation 25: Covariance matrix



# 6 Results and discussion

The result in this thesis is heavily dependent on simulations due to no access to the interferometer at the end of the semester. There are some tests done on data from the interferometer, but this is data obtained week beforehand and not “live” data. These datasets can be imported in Matlab and then run it through Simulink which is done in 0 below. These datasets are obtained heating up the aluminium rod and doing

## 6.1 Simulation

The simulations are done in Simulink with Jones calculus as explained in 3.1. There has been tested several different state space models, but the one explained in 5.1 have shown the best results, this could be better since that algorithm only remove the gain bias and don't compensate for the amplitude gain in the two output signals. However, when using the arctangent to get the angle this won't really matter since the angle is the ratio between the two signals and therefore will be the same no matter their gain.

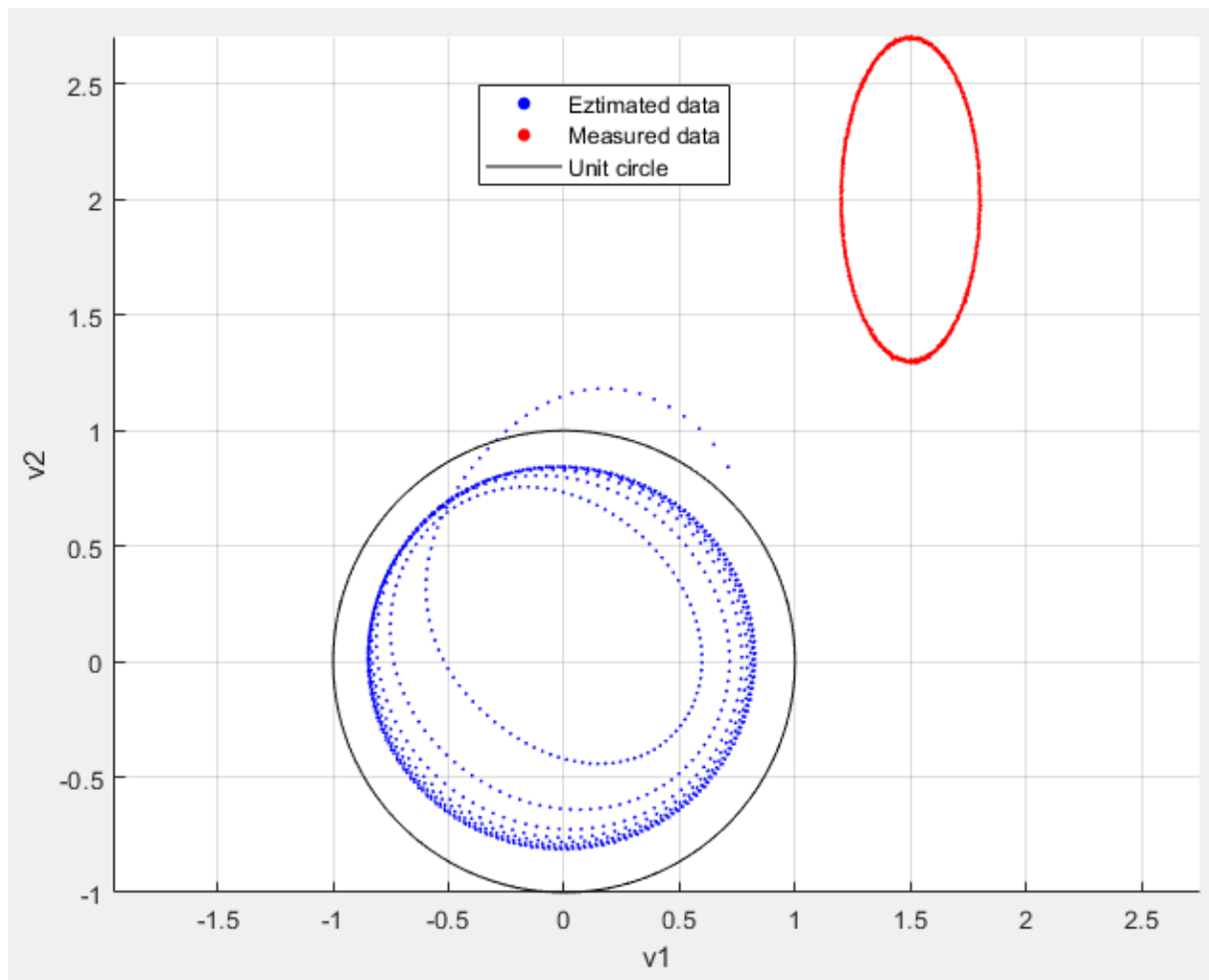


Figure 8: Simulated data with noise and estimated data

As shown in Figure 8 the estimated data will form a circle around origin. The angle we then need to calculate for the movement of the TM is given by  $\varphi = \text{atan}\left(\frac{v_2}{v_1}\right)$ . The moved distance of the mirror is then

$$\Delta L = \frac{\varphi}{2\pi} \cdot \lambda$$

Before calculating  $\Delta L$  an unwrapping must be done to avoid the characteristic spiky stairs the arctangent function will make.

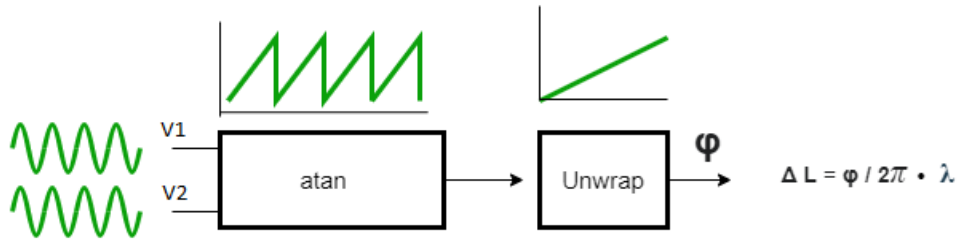


Figure 9: Unwrapping of the two output signals (Nesjø & Kvamme, 2021)

Figure 10 shows that the result of the calculation of  $\Delta L$  will be the same with just removing the bias in amplitude and not placing the estimated data on the unit circle. Figure 10 is the last 100 samples of the same simulation in Figure 8 of 1501 samples. This is when the states have stabilized and will give a good a result. If we look at the first 250 samples of the same data, it is clearly that the estimated data is diffused and need some time to stabilize. This is shown in Figure 11 and can also be seen in Figure 8.

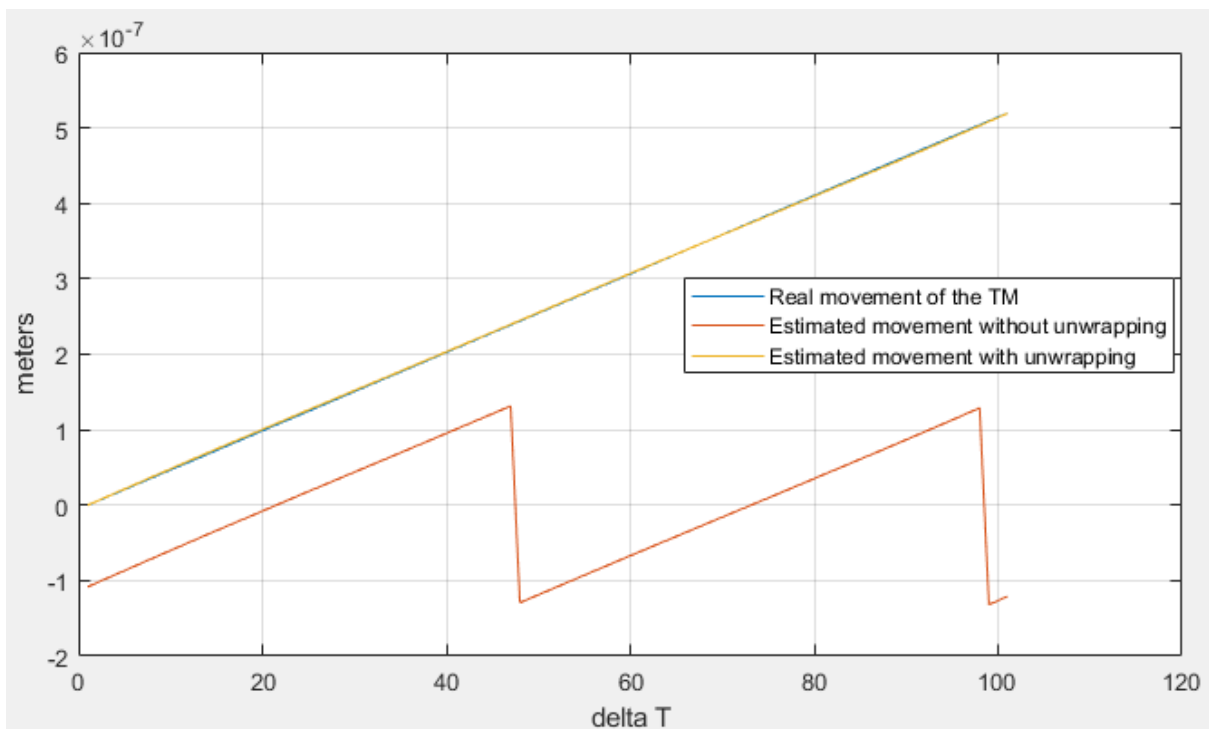


Figure 10: Last 100 samples for  $\Delta L$  of the data in Figure 8, with and without unwrapping

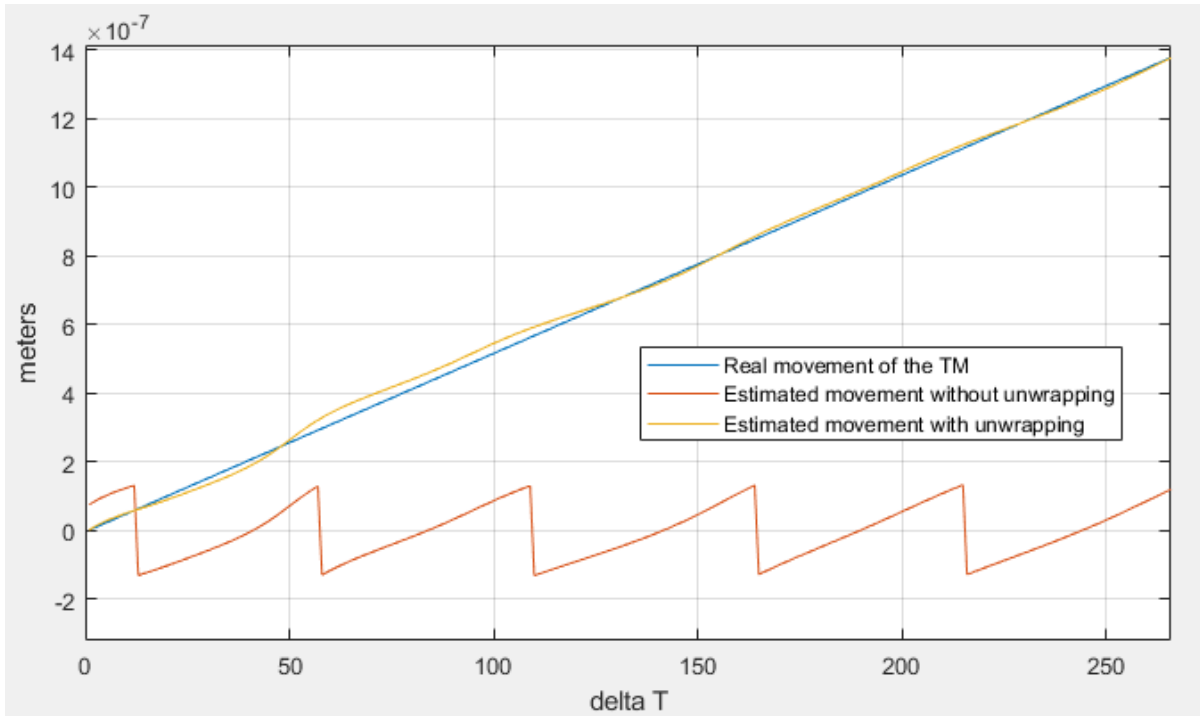


Figure 11: First 250 samples for  $\Delta L$  of the data in Figure 8, with and without unwrapping

The offset in the two signals are well estimated and can be seen in Figure 8 by how the circle is placed around origin. The estimated value of  $\alpha_1$  and  $\alpha_2$  will converge to their real values over time and this is shown in Figure 13. The same figure also shows that it will be quicker with the right initial values where the initial value of  $\alpha_2$  is different from the top and bottom part of the figure. A higher covariance value for  $\alpha_1$  and  $\alpha_2$  also makes it quicker, but this will also make the estimate oscillate more. That's why low covariance values are presented in Equation 25: Covariance matrix.

When it comes to the initial values usually a good guess is using the mean of the state. The mean of the displacement states is unknown, but we can make a good guess from what we know.

The mean of  $x_1$  and  $x_2$  is zero since they should be cosine and sine functions. The mean of  $\alpha_1$  and  $\alpha_2$  should be more than one since the photodetectors won't give a negative output, how much more than zero depends on the environment the interferometer is placed in. A dark room will here give a lower value than a light up room because the photodetectors receive more light from the environment. For the mean of  $\beta_1$  and  $\beta_2$  this should be one if an amplifier circuit with the right gain is used. In this case it will be something different since  $\beta_1$  and  $\beta_2$  are only used to estimate the amplitude bias.

$$\begin{aligned} \hat{x}_1(0) = E\{x_1(0)\} = 0 & & \hat{x}_2(0) = E\{x_2(0)\} = 0 \\ \hat{x}_3(0) = E\{\beta_1(0)\} = 1 & & \hat{x}_4(0) = E\{\beta_2(0)\} = 1 \\ \hat{x}_5(0) = E\{\alpha_1(0)\} > 0 & & \hat{x}_6(0) = E\{\alpha_2(0)\} > 0 \end{aligned}$$

Figure 12: Guesses for initial values of the states

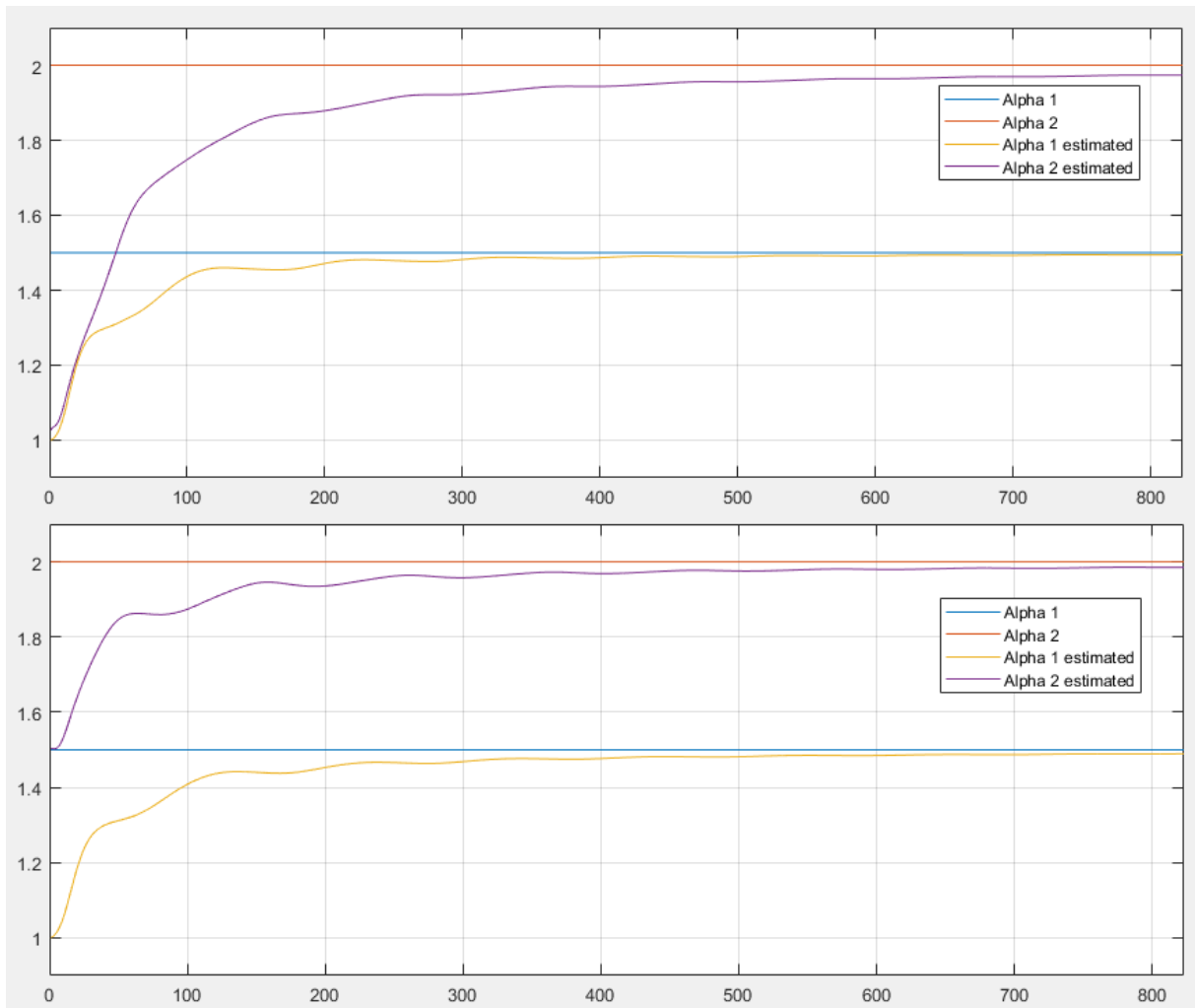


Figure 13: Different initial values for  $\alpha_1$  and  $\alpha_2$  and how they stabilize over time

## 6.2 Using actual data

Using a USB-6001 (National Instruments, n.d.) analog-to-digital converter connected to the oscilloscope the signals from the photodetectors can be stored on a computer through Matlab. This data is then used in Simulink to do test results.

The error in the waveplate were removed manually by removing some of the first samples in the sine vector because the aluminium rod is moving smoothly and gives sinewaves as outputs. This is not the right way to do it in a live setup since the aluminium rod may move at different speed or move back and forth. It is done this way only for demonstration purposes for a scenario where the quadrature error is removed. The right way would probably be to add a constant to the arcsine of the measured signal, but in this case the methods will be the same.

The actual movement of the rod is unknown, so there is no way of knowing if the measurement is correct. Therefore, the EKF algorithm is compared to the Heydemann method (3.2).

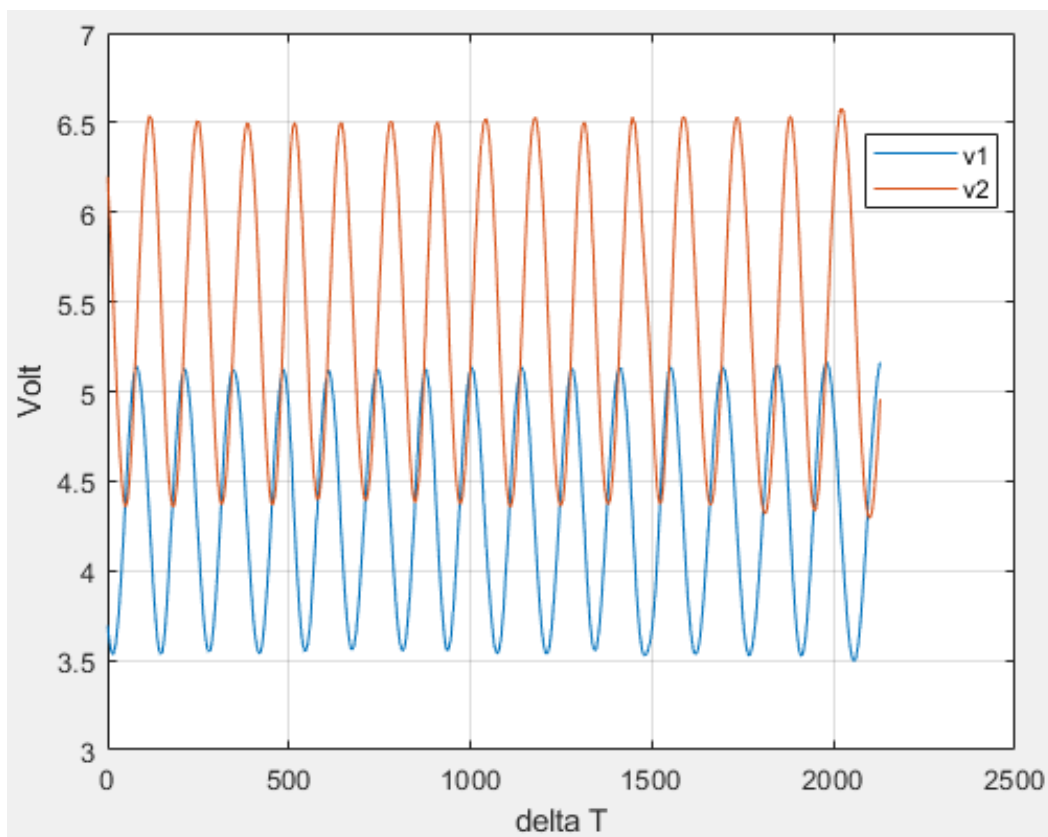


Figure 14: Measured data used in this demonstration

The measured data is shown in Figure 14 and if the initial states were too far off the system will diverge. This were pushed to its limits to have a good demonstration of how they will stabilize over time. The stabilisation that happens can be easily seen in Figure 15 and Figure 16 on the next page. Although Figure 15 don't look pretty it gives good results in the end.

As in the simulation the amplitude is not compensated for, but this won't be a problem when unwrapping done in Figure 16.

Compared to the Heydemann method (Figure 16) the start is a bit of, but after a while when stabilized, the results shows a smoother progress. Assuming that the movement of the aluminium rod is not oscillating, the EKF algorithm gives a much better result than the Heydemann method when stabilized. The oscillation in the two methods are more easily represented when looking at their derivatives. This is done in Figure 17.

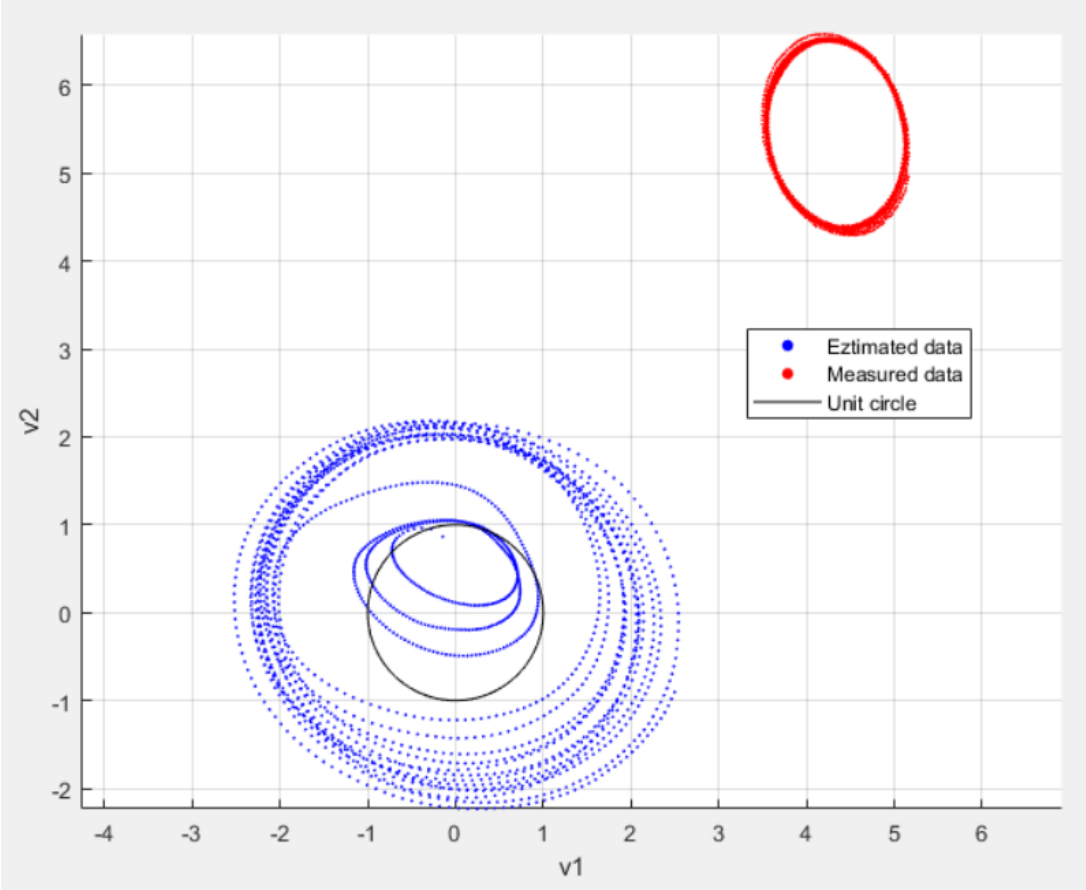


Figure 15: The output signals plotted up against each other

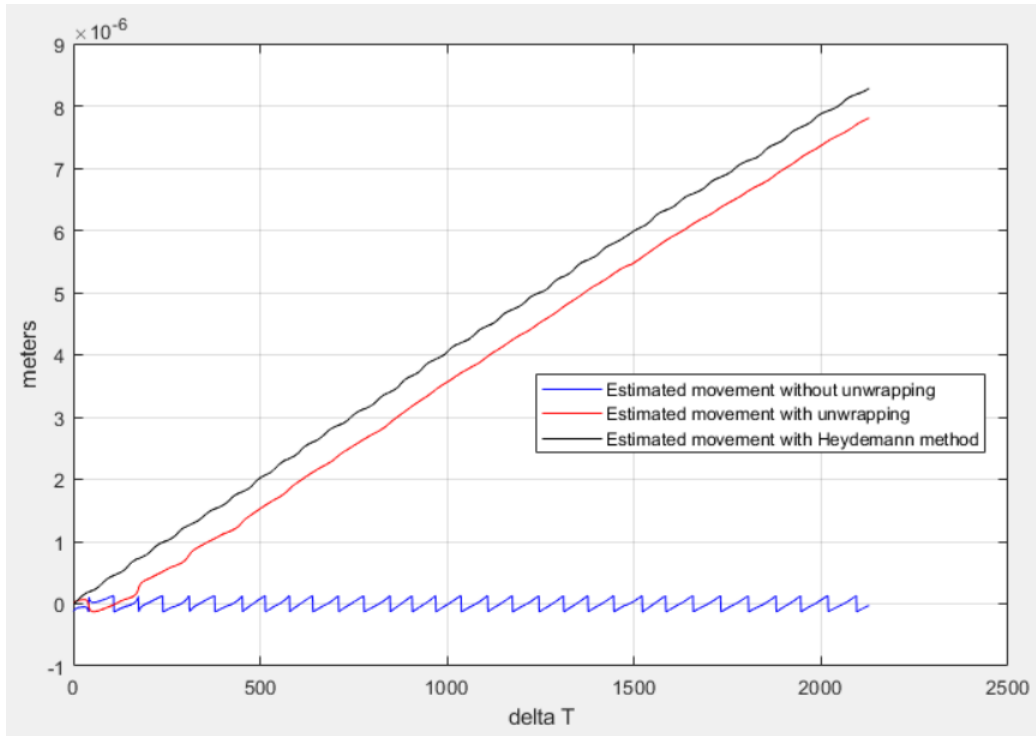


Figure 16: Estimated movement with both the EKF algorithm and the Heydemann method

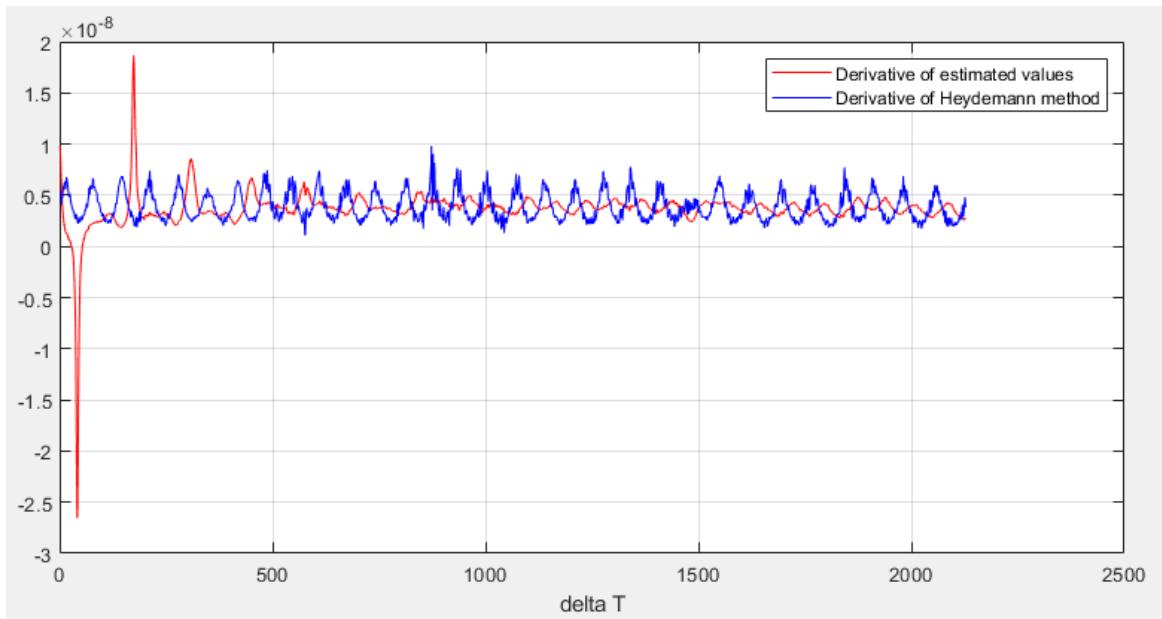


Figure 17: The derivatives of the estimated values using EKF and the Heydemann method

### 6.3 Real-time implementation

A real-time setup has not been done in this project, but since MathWorks have made it easy to generate code from the EKF Simulink block, together with the analog-to-digital converter from National Instruments USB-6001 (National Instruments, n.d.), this should be rather easy to do. The code can be generated in both C and C++ code.

# 7 Conclusion

The last years there has been focus on live displacement estimation of interferometric noise. A set of different estimation methods has been tested with different outcome. For instance, in Petter Ersbo's master thesis (Ersbo, 2018) the particle filter has been used for estimation. The particle filter needs a lot of computer power to operate and therefore an Extended Kalman Filter (EKF) has been used for estimation in this paper.

The Simulink model based on Jones calculus (4 Model and simulation) has been crucial for implementing an EKF because using the interferometer takes a lot of time to calibrate and the actual values that are measured is unknown. The model made has shown to be a good representation of an interferometer in real life. The model itself need some computer power to run the simulations, but the EKF block used won't add any noticeable time to this.

The state space model used gives both good and bad results and need some improvements. The measurements obtained is done by heating up metal which gives a constant movement of the target mirror in one direction, and therefore the EKF is designed accordingly. Some other type of measurement might cause trouble. There is also some instability in the filter if the initial values are too far off or if the covariance matrix is not tuned right. But if this is done right the filter works fine.

The displacement away from origin is well estimated as shown in Figure 13, but the amplitude gain is not. This has been compensated instead to estimate the amplitude bias so that when taking the arctangent this don't really matter. Ideally the amplitude should also be estimated. There is also the error in the quadrature signal. This has shown to be hard to estimate but is often not changing much and has therefore been assumed as a constant.

When looking at the final results it seems that the estimation using EKF gives a better and more precise estimate than the Heydemann method, this need of course more testing before proven and is just an assumption as long as the actual movement of the metal is unknown. There is also always an uncertainty in the laser wavelength, which this approach is not able to estimate due to its dependency of a known wavelength. To do testing of high accuracy to verify the results in a real-time setup, better equipment needs to be used. The laser wavelength is not accurate enough and there is no isolator in this setup. The waveplate is also not ideal.

What this paper do prove is that there is possible by using an EKF to estimate displacement noise on a homodyne Michelson interferometer, but it need some more work.

For future work a better state space model might be obtained and a model with estimates of the amplitude gain and the quadrature error. There might be better using the EKF with a state space model that has a totally different approach than in this paper and it would be interesting to see what approaches could be used. A real-time setup should also be possible to do but might need some extra software or equipment. This has not been investigated at the end of the semester due to no access to the interferometer.



# 8 Bibliography

- (2021). Retrieved from MathWorks: <https://se.mathworks.com/help/fusion/ug/extended-kalman-filters.html>
- Eielsen, A. A. (2018). *Notes on Displacement Interferometry*.
- Eielsen, A. A. (2021, January). Improved displacement estimation in homodyne Michelson interferometers (Project description for this thesis).
- Ersbo, P. (2018). *Displacement Estimation for Homodyne Michelson Interferometers Based on Particle Filtering*.
- Hecht, E. (2001). Optics (3rd ed.). Retrieved from <https://archive.org/details/optics00ehec/page/n383/mode/2up?q=jones>
- Heydemann, P. L. (1981). *Determination and correction of quadrature fringe*. Peter L. M. Heydemann. Retrieved February 2021, from <https://www.osapublishing.org/ao/abstract.cfm?uri=ao-20-19-3382>
- LIGO Caltech. (n.d.). Retrieved June 26, 2021, from <https://www.ligo.caltech.edu/>
- LIGO's Interferometer. (n.d.). Retrieved June 26, 2021, from <https://www.ligo.caltech.edu/page/ligos-ifo>
- Loughridge, R., & Abramovitch, D. (2013, June). A Tutorial on Laser Interferometry for Precision Measurements.
- National Instruments. (n.d.). Retrieved from <https://www.ni.com/documentation/en/multifunction-io-device/latest/usb-6001/overview/>
- Nesjø, T., & Kvamme, M. (2021, May 15). Improved displacement estimation in homodyne Michelson interferometer.
- Simon, D. (2006). *Optimal State Estimation*. John Wiley & Sons, Inc.
- Thorlabs. (n.d.). Retrieved July 1, 2021, from [https://www.thorlabs.com/\\_SD-Popup.cfm?partnumber=EDU-MINT2](https://www.thorlabs.com/_SD-Popup.cfm?partnumber=EDU-MINT2)